Slipping SLIP Template

Gargi Sadalgekar Jian Kwon Kapi Ketan Mehta

***Abstract*—The Spring Loaded Inverted Pendulum (SLIP) model has been widely used as a template to explain dynamic running of human and animals. However, the SLIP model operates under a no-slip constraint. Slippage is an essential aspect of maneuvering for many biological systems, but there has been little work done on incorporating slippage to the SLIP model. In this paper, we demonstrate that the conventional SLIP model fails with low friction and propose an alternative dynamic model, Slipping SLIP. We also provide a GAZEBO simulation environment with the RHex robot for robot locomotion research.**

I. Introduction

Running animals and robots can be modeled using the Spring Loaded Inverted Pendulum (SLIP) template [1]. The SLIP template describes sagittal plane locomotion and compliant legged locomotion quite accurately. As the result, the model widely has been used as a good starting point for understanding and studying control and mathematical theory of robots with compliant legs.

The RHex robot [2] is a hexapod robot inspired by cockroaches. Its design consists of of a rigid body with six compliant legs (3 on each side), each with a singular rotational degree of freedom [3]. [2] verifies that RHex's dynamics can be approximated using the SLIP model for running. However, the SLIP model assumes that there is no slip in the system. If we are to extend the model to higher dimensions of motion, it is possible that the dynamics will diverge from the SLIP model's predictions since maneuvering in 2+ dimensions is impossible without slipping, as previously established. Therefore it will be useful to modify the standard SLIP-model to incorporate slippage [4] and then model the RHex's dynamics in two dimensions by steering it in the horizontal plane.

The RHex, like most low DoF multi-legged robots, accomplishes its high maneuverability via slipping. [5] demonstrates that, much like with actual cockroaches, in order for steering to be possible, slipping must occur. This paper defines steering as the ability to turn continuously with magnitudes of turn in an interval containing 0 while at the same time also translating (this is distinct from turning as one can turn in place but not steer in place). While there are examples ([6], [7]) which demonstrate that steering a RHex is achievable, they do not incorporate slippage in their models. Various friction models [8] [9] [10] [11] [12] exist which are able to represent friction in different phases and could be used to represent such forces in the SLIP system. We can then compare the dynamics predicted by the modified SLIP model to experimental data from steering a RHex over a flat surface.

[4] analytically shows that when the original SLIP model is allowed to slip, the system is unstable and cannot recover after slipping. It proposes a new SLIP model, called the TDMF-SLIP, that incorporates a small point mass at the foot of the leg and has stable limit cycles.

We propose an alternative model, called the slipping SLIP model, consisting of 2-link leg with a torsion spring at the knee and a small point mass at the foot.

II. Friction and the Original SLIP Model

A. The Original SLIP Dynamics Model

The SLIP model for running consists of a point mass, M, attached to a massless spring leg with stiffness k and rest length l_0. The leg is parameterized by its length, r, and its angle from vertical, θ. The motion of the model is split into two phases: flight and stance. The stance phase begins when the spring comes in contact with the ground. The spring compresses and exerts a force of $k(l_0 - r)$ on the point mass in the outward radial direction. When the spring returns to its rest length ($r = l_0$), the spring lifts off the ground and the system enters the flight phase. In the flight phase, the point mass enters ballistic flight, with gravitational force, Mg, being the only force acting on it. When the spring comes back into contact with the ground, the leg sticks, and the system re-enters the stance phase. It is assumed that the contact point between the spring and the ground is fixed during stance phase, and that the spring remains at a fixed length and angle, r and $\theta = \theta_0$, during flight. θ_0 can also be considered as the attack angle, as it is the orientation of the leg when the spring contacts the ground.

The dynamics of the SLIP model are as follows:
Flight:

$$\ddot{x_M} = 0 \tag{1}$$

$$\ddot{y_M} = -g \tag{2}$$

Stance:

$$\ddot{r} = r\dot{\theta}^2 - g\cos\theta + \frac{k}{M}(l_0 - r) \tag{3}$$

$$\ddot{\theta} = \frac{-2}{r}\dot{r}\dot{\theta} + \frac{g}{r}\sin\theta \tag{4}$$

Figures 1 and 2 visualizes the SLIP model parameters and its motion

B. Introducing Friction to the SLIP model

We can analyze the impact of slippage on the SLIP model by introducing friction as a parameter of the system, and then adjusting it to allow for slippage. For this paper, we elected to use the Coulomb friction model because it is one of the

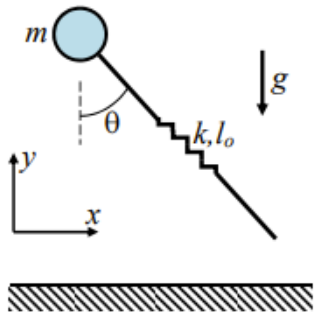

Fig. 1. SLIP model parameters [4]

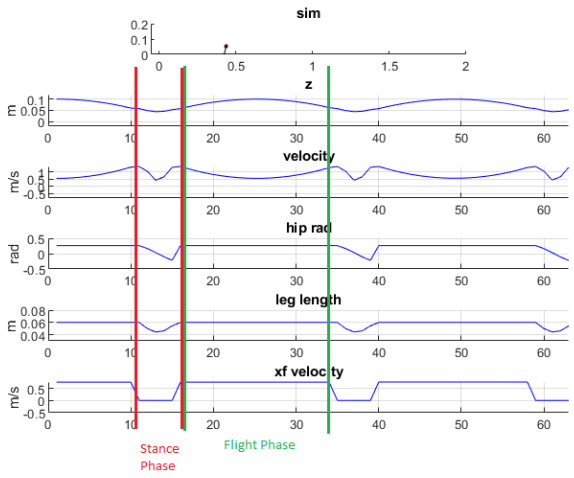

Fig. 2. SLIP model dynamics for a high friction system (no slippage). From top to bottom the plots show: the height of the point mass, the net velocity of the point mass, the orientation of the leg, the length of the spring, and the velocity of the foot all vs time. The red section shows the behavior during stance phase, and the green section shows the behavior during flight phase

simplest to execute. According to the Coulomb friction model [13], the friction force acting on a point can be defined as

$$F_{fr} = \mu F_N \text{sign}(v) \tag{5}$$

where F_N is the normal force, and v is the velocity of the point (see Fig. 3).

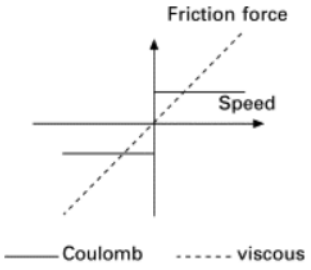

Fig. 3. Coulomb friction model [13]

In general, slippage occurs when the horizontal force, F_x, is greater than the friction force. For the SLIP model, F_x and F_N are functions of the force exerted by the spring onto the ground F_{spr}, where

$$F_x = F_{\text{spr}} \sin\theta \tag{6}$$
$$F_y = F_{\text{spr}} \cos\theta \tag{7}$$
$$\tag{8}$$

Therefore, in order for the leg to stick when the model enters the stance phase, we arrive at the following condition on the leg's attack angle:

$$|F_x| < F_{fr} \tag{9}$$
$$|F_{\text{spr}} \sin\theta| < \mu F_{\text{spr}} \cos\theta \tag{10}$$
$$|\tan\theta| < \mu \tag{11}$$

Physically, this means that the leg orientation has an allowable range of $2\arctan(\mu)$ about the vertical, within which the leg will not slip. By doing a simple force comparison (Fig. 4) we can also confirm that under the Coulomb friction model that once the leg slips, it cannot re-stick as the forward force from the spring overtakes the backward from friction.

Furthermore, we can account for the energy lost upon impact with the ground by placing a similar condition on the velocity of the foot $(\dot{x_f}, \dot{y_f})$ immediately before impact with the ground. In order for a perfectly inelastic collision to occur (which would lead to the foot sticking to the ground instead of slipping) the following limitation arises:

$$|\dot{x_f}| \leq \mu |\dot{y_f}| \tag{12}$$

If this condition is met, then the horizontal velocity of the foot instantaneously drops to 0 after making contact with the ground. If it is not met then the post-impact horizontal foot velocity is defined as

$$\dot{x_f}_{\text{post}} = \dot{x_f}_{\text{pre}} - \mu \text{sign}(\dot{x_f}_{\text{pre}}) |\dot{y_f}| \tag{13}$$

and the system slips directly upon impact.

[4] establishes that the original SLIP model will fail to recover after slipping because the spring is massless. It assumes that when the point of contact between the spring and the ground is free to slip horizontally, it will move with infinite acceleration while upper point mass is stationary. This results in an instantaneous extension of the spring until it reaches its rest length, l_0, at which point the spring loses contact with the ground and the model falls. We empirically confirmed this by adding a small point mass to the foot of the spring, $m_f << M$, and allowing its mass to approach 0. Fig. 5 shows the comparison of the two systems. Table I shows the parameters used for the simulation. Note that the coefficient of friction for the low friction simulation is exactly $\mu_{lf} = \tan(\theta_0)$. This makes the model enter the stance phase exactly on the threshold of the slip condition (Eqn 11).

We can see in Fig. 5b that as $m_f \longrightarrow 0$, the system slips and does not recover when there is not adequate friction. In the first stride, the foot's velocity doesn't reach 0 during stance

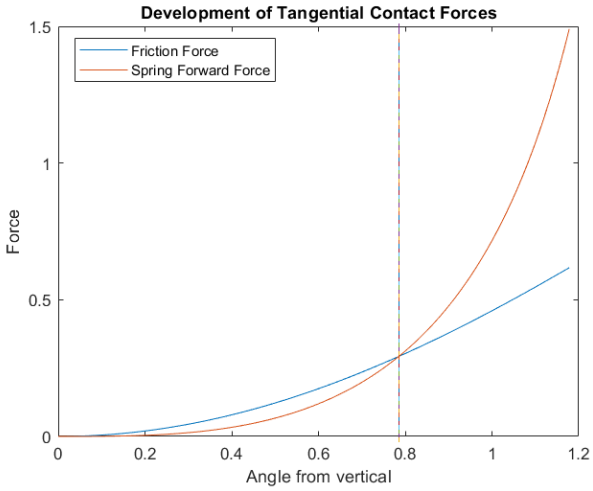

Fig. 4. Development of horizontal component of spring force and friction force as a function of θ. There vertical line represents the slipping threshold $\theta = \arctan(\mu)$.

TABLE I
SLIP SIMULATION PARAMTERS

Parameter	Parameter Variable	Value
Point Mass	M	0.1 kg
Foot Mass	m_f	1e-4 kg
Spring Rest Length	l_0	0.06 m
Spring Stiffness	k	500
Leg Angle of Attack	θ_0	$\pi/12$ rad
Coefficient of Friction for Low Friction Sim	μ_{lf}	0.2679
Coefficient of Friction for High Friction Sim	μ_{hf}	1e6

phase, indicating slippage. This causes an energy loss which results in deterioration of the following strides. In contrast, when the friction is significantly large, the system is able to achieve a stable gait, regardless of the mass of the foot.

This simulation verifies that the original SLIP model is unable to model systems where simulation occurs.

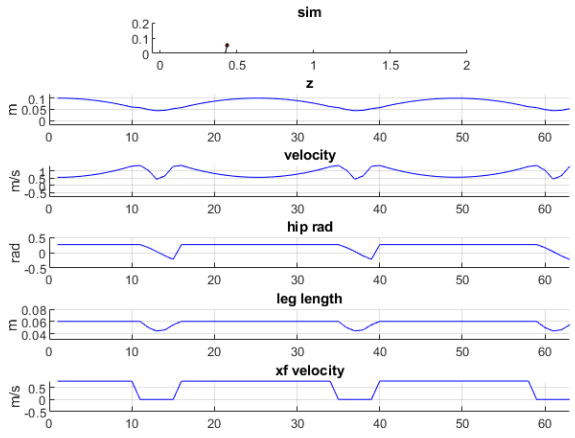

(a) High friction

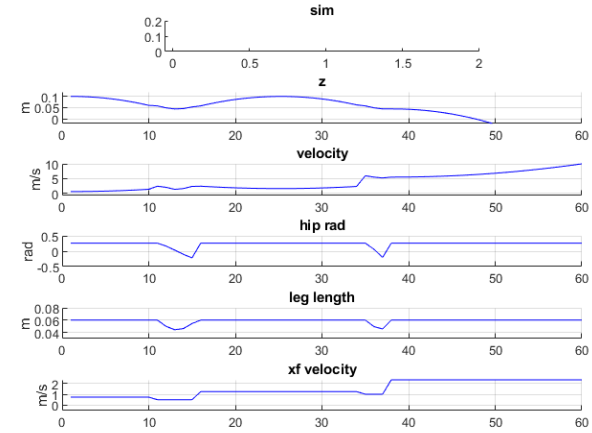

(b) Low Friction

Fig. 5. Comparison of SLIP behavior as friction decreases

III. Friction and the Segmented Leg SLIP model

A. The Original Segmented Leg Model

The segmented leg model consists of a point mass, M, attached to leg made of 2 massless links, with links of lengths l_1 and l_2 respectively. The two links are connected by a torsion spring with stiffness k and rest angle θ_0. We refer to this connection between the links as the knee, and the connection between the point mass and the upper link as the hip. Similar to the SLIP model, the segmented leg model has two phases, flight and stance. The dynamics and behavior of the flight phase are the same as those of the SLIP model. The stance phase occurs when the lower link makes contact with the ground. The torsion spring compresses and exerts a torque $\tau = k(\theta_0 - \theta)$ upward on the point mass. When the spring returns to its rest angle and the resultant force at the foot becomes zero, the leg loses contact with the ground and the model enters the flight phase. All assumptions from the SLIP model are applied to this model as well. For the purpose of this paper, we assume that $l_1 = l_2 = l_0$. Figure 6 visualizes the model and its parameters.

The dynamics of the stance phase of the segmented leg model derived from force-torque balancing are as follows:

$$\ddot{x} = -\frac{\tau}{Ml_0 \sin\alpha} \cos\psi \tag{14}$$

$$\ddot{y} = \frac{\tau}{Ml_0 \sin\alpha} \sin\psi - Mg \tag{15}$$

We first verify that the segmented model dynamics match that of the original SLIP model. The hypothesis is that the 2 segment leg model could replicate the dynamics of a simple SLIP model and can be generalized for a more realistic models. The dynamics of the SLIP model and Segmented Leg model are qualitatively similar(see Fig 7)

The segmented leg model is more sensitive to small changes in initial conditions and system parameters. Most of the fixed points found were unstable and would make the system unstable from small perturbations.(See Fig 8) The

unstable nature of the fixed points were found through the poincaré section analysis with initial height as the poincaré section and the return map was numerically calculated for each initial point. Majority of the initial points were not able to intersect the section but the few points which did were unstable or unstable fixed points.
The eigenvalues of the return map of the system at one of such fixed points were as follows:

Fixed Point: $\begin{bmatrix}1.46 & 1.6358\end{bmatrix}$

Jacobian: $\begin{bmatrix}3.32325 & -0.2994\\ -0.34577 & 1.04456\end{bmatrix}$

Eigenvalues: $\begin{bmatrix}3.36781 & 1.0000\end{bmatrix}$

Eigenvectors: $\begin{bmatrix}0.98910 & 0.12781\\ -0.147209 & 0.991798\end{bmatrix}$

The eigenvalues of the return map are all positive hence the system is unstable and cannot recover from perturbations. But interestingly, one eigenvalue always assumes the value of 1 with every fixed point found. Such is the case because the system does not simulate the heel strike and the spring is assumed to store and return all the energy stored back into the system hence the energy of the system remains constant. The eigenvectors are not diagonalized hence we cannot directly assign eigenvalues to the initial condition parameters.

B. The Segmented Leg Model with a Foot Mass

The segmented leg model is attached with a small mass at the foot with the original parameters intact. The mass is added to derive equation of motion for the foot to analyze the effect of friction force limitation on the foot location.

The derivation of the equation starts with setting up an convenient coordinate system. Unlike the original segmented leg model, the system state $[q_1 q_2 q_3 q_4]$ where q_1 is the angle of the upper link to the vertical, q_2 is the angle between the two two links, q_3 is the x position of the foot and q_4 is the y position of the foot.(See Fig 9)

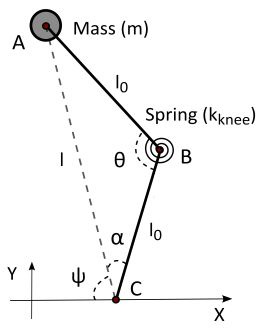

Fig. 6. Segmented leg model. The line from the foot contact to the mass divides the angle between ground and the lower leg segment into the angles α and ψ. l is the total leg length from foot contact to the point mass [14]

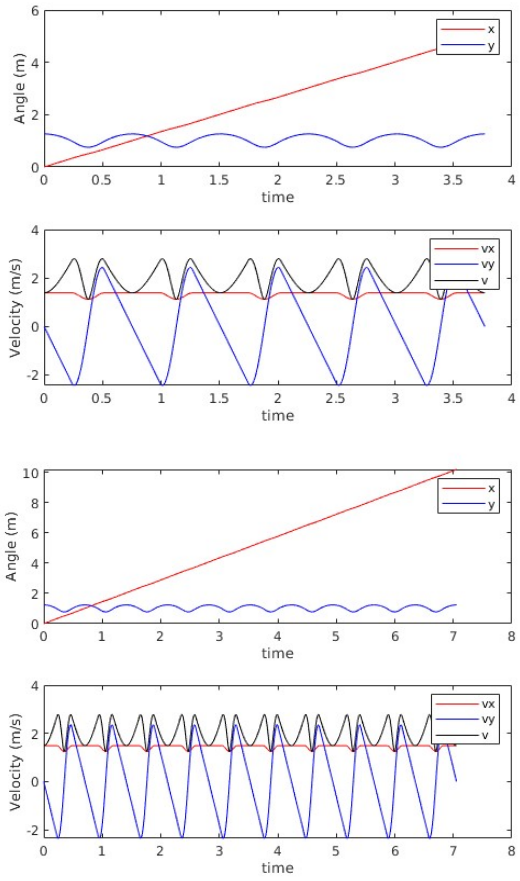

Fig. 7. The velocity of a segmented leg qualitatively follows the dynamics of a SLIP model. The torsion spring acts more linearly for small changes in the knee angles. Top (1st and 2nd plot): Segmented Model Dynamics, Bottom (3rd and 4th plot): SLIP Model Dynamics

From here, we use Lagrange's equations to derive the following state dynamics:

$$\begin{aligned}&-gl_1M\sin(q_1)+gl_2M\sin(q_2-q_1)+\\ &\quad\ddot{q_1}\left(l_1^2M+2l_1l_2M\cos(q_2)+l_2M\right)-\\ &\quad2l_1l_2M\dot{q_1}\dot{q_2}\sin(q_2)-l_1l_2M\ddot{q_2}\cos(q_2)+\\ &\quad l_1l_2M\dot{q_2}\sin(q_2)+\\ &\quad l_1M\ddot{q_3}\cos(q_1)+l_2^2(-M)\ddot{q_2}+\\ &\quad l_2M\ddot{q_3}\cos(q_2-q_1)=0\end{aligned} \tag{16}$$

$$\begin{aligned}&-gl_2M\sin(q_2-q_1)+k(q_2-\theta_0)-l_1l_2M\ddot{q_1}\cos(q_2)+\\ &\quad l_1l_2M\dot{q_1}^2\sin(q_2)-l_1l_2M\dot{q_1}\dot{q_2}\sin(q_2)+\\ &\quad l_1l_2M\dot{q_1}\dot{q_2}\sin(q_2)+l_2^2(-M)\ddot{q_1}+\\ &\quad l_2^2M\ddot{q_2}-l_2M\ddot{q_3}\cos(q_2-q_1)=0\end{aligned} \tag{17}$$

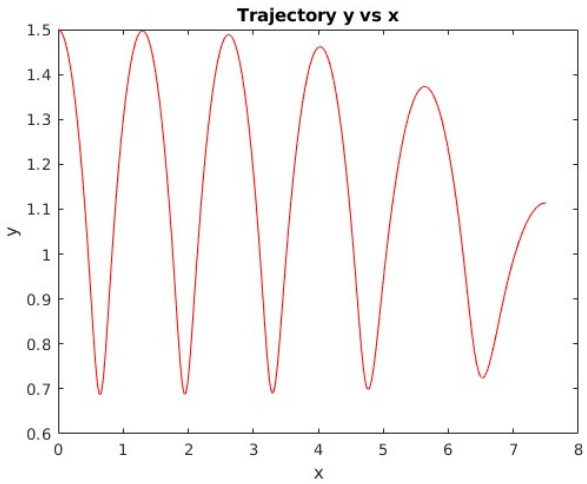

Fig. 8. The fixed point found was v_{x0}=1.46 and y_0=1.6357 and the initial point for the system was v_{x0}=1.45 and y_0=1.5. Small perturbation of order -2 made the system unstable.

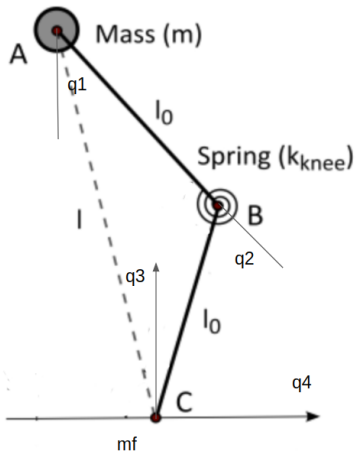

Fig. 9. The coordinate setup.

$$l_1 M\ddot{q_1}\cos(q_1) - l_1 M\dot{q_1}^2\sin(q_1) + l_2 M\ddot{q_1}\cos(q_2 - q_1) + \tag{18}$$
$$l_2 M\dot{q_1}^2\sin(q_2 - q_1) - 2l_2 M\dot{q_1}\dot{q_2}\sin(q_2 - q_1) -$$
$$l_2 M\ddot{q_2}\cos(q_2 - q_1) + l_2 M\dot{q_2}^2\sin(q_2 - q_1) +$$
$$\ddot{q_3}(M + m_f) = F_x$$

These equations were then solved to isolate the state parameters and to verify that the system is indeed solvable. For simplicity when simulating, we eliminated $q(4)$ and its corresponding terms and equation by assuming that during stance phase, the foot will always remain in contact with the ground.

The system like the original model will have two phases- flight and stance. The flight phase is same as for every model with massless links. For the flight to stance transition, the dynamics depends on the velocity at the touchdown and depends on the equations $(9) - (11)$.

Further during the stance the force exerted by the leg on the ground needs to be checked that the horizontal force component increases beyond the highest friction force possible between the surfaces and the sliding friction equivalent comes into action where the friction force becomes constant and equal to the maximum value of the static friction.

The system is closer to the reality but is difficult to find a fixed point numerically due to instability because of the falling and slipping events where the system of equations can become invalid when it leaves the ground.

IV. SLIP IN SIMULATION

A. Test Platform: RHex Robot

The RHex maneuvers via an "alternating tripod gait" where 3 of the RHex's legs (1 on one side and 2 on the other) contact the ground during each stride. This gives the system passive dynamic stability which allows it to traverse complex terrains easily. RHex's agility and maneuverability has allowed it to be used widely as a testing platform for locomotion and control [15].

Due to these reasons, we choose the RHex as our test platform. We conducted first experimental using simulation environment with non-slip condition (high friction).

B. Simulation Environment Setting

The simulation performed in GAZEBO with Robot Operating System(ROS). Physical properties of the RHex robot, such as inertia, mass and coordinates, defined and calculated using sw_urdf_exporter at Solidworks. We also can change the robot ground contact friction in GAZEBO. Since the

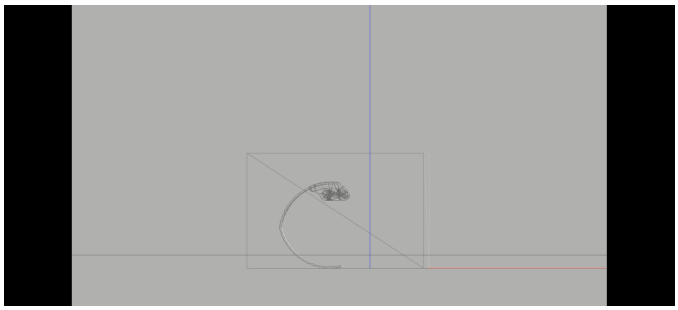

(a) Compressed.

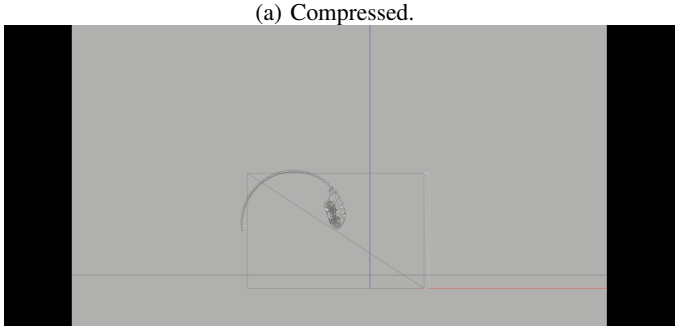

(b) Leased.

Fig. 10. Compliance leg.

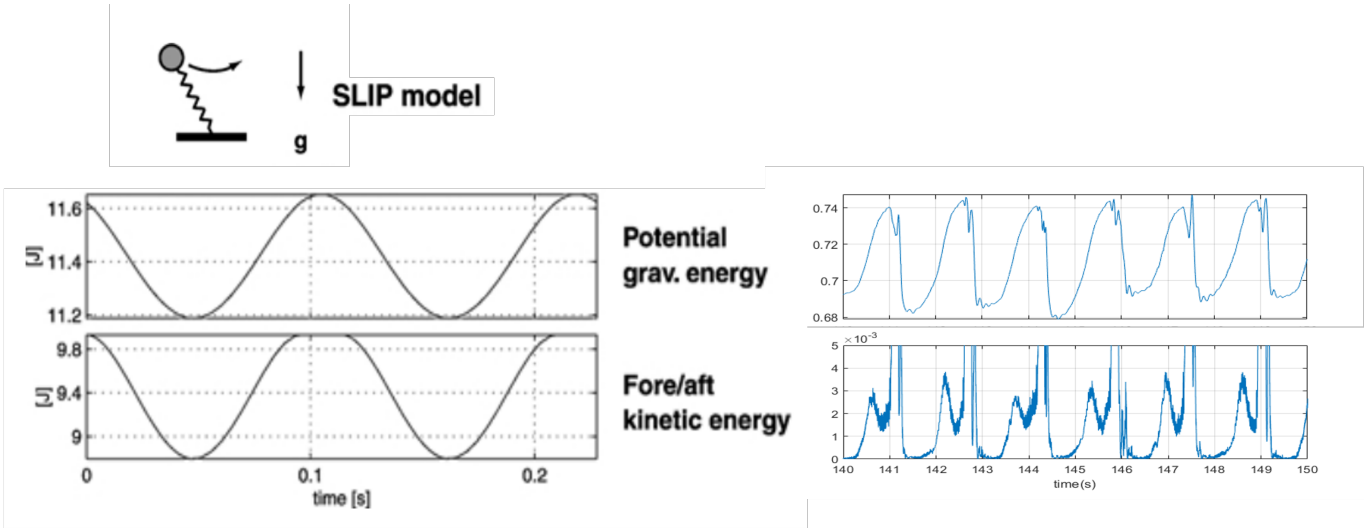

Fig. 11. Comparison of (left) theoretical SLIP predictions [16] with (right) RHex simulation data.

every element are considered as rigid in GAZEBO, the C-shape leg of the RHex is cut at the middle position of the C and a spring-like joint added at that position. Due to difficult making Simulation Environment same as real world, many parameters, such as spring constant and friction, are fitted to derive the ideal experiment result. As the result, we achieved elastic property at the legs in the simulation environment. (Fig. 10)

After verification with single leg, all the other legs were also changed to the compliance leg. The robot is controlled by position trajectory based on a Buehler clock. The Flight phase is from 330° to 30° rotation angle and The Stance phase is from 30° to 330° rotation angle. The signal frequency is 50Hz.

C. Verification of SLIP in RHex Simulation

A Previous work [2] verifies that RHex's dynamics can be approximated using the SLIP model for running. To validate our simulation platform, the position and velocity of center of the mass are collected and compared with theoretical result in Fig. 11. Also, the friction is set very high same as SLIP model. The Y-axis label of the simulation data graph is omitted, since our simulations parameters are not realistic.

The SLIP predictions graph(Fig. 11 left) is about one stride and the simulation result graph(Fig. 11 right) is about multiple stride, approximate five strides. The data shows that potential and kinetic energy has same phase as the SLIP predictions. This result verifies that the simulation anchors with SLIP predictions.

One characteristic to note is that the kinetic energy shows 'M' shape behavior. It also observed human running data. This seems because the RHex maneuvers with two tripod gait, alternating tripod gait.

V. Discussion and Future Works

We proved that SLIP model fails to deal slippage, discussed about a method to analyze slippage in a system and presented that 2 segmented model simulation anchor SLIP model and can be extended for analyzing a slipping foot in theory.

The response of the simple SLIP model shows a characteristic graph of the model which has been studied for years now. Adding slippage makes the system more real and the simulation shows that once the SLIP model starts slipping, the system cannot recover. Such dynamics is expected of the anchor template model since the system does not have a mechanism to recover from spring force exceeding the friction force event. For a recovery mechanism model, the 2 segmented leg model is an ideal case. Ideally, the leg has the capability of adjusting the force through bending the knee and still reaching a state which allows further steps. The response from the natural dynamics of the segmented model is similar to the SLIP model but is more sensitive to initial conditions for a stable periodic motion. Although the segmented model can be a better anchor for the RHex legs. The simulation response graph qualitatively follows the SLIP response but has unsual valleys which are suspected to be due to the leg-ground collision or more ideally called "heel-strike" event and the hip actuation of the legs. Considered the leg-ground collision and the hip actuation is modelled in the segmented leg, the response from such a model could be closer to the response from the physics of the simulation than a simple SLIP model.

For the future works, the 2 segment model dynamics has to be simulated to find a stable fixed point and similarly with the slipping foot. We can compare new dynamic model result with RHex simulation with lower friction environment and study the new dynamic model representation of SLIP model with slippage. Moreover, the model could be extended to study the performance of multiple legs based on the model beside the real world data. Also, our parameters in simulations are far from real world values and stable and needs to be tuned to match the real world stable dynamic system responses.

REFERENCES

[1] H. Geyer, U. Saranli, A. Goswami, and P. Vadakkepat, "Gait based on the spring-loaded inverted pendulum," in *Humanoid Robotics: A Reference*. Springer Netherlands, 2018, pp. 1–25.

[2] R. Altendorfer, N. Moore, H. Komsuoglu, M. Buehler, H. Brown, D. McMordie, U. Saranli, R. Full, and D. E. Koditschek, "Rhex: A biologically inspired hexapod runner," *Autonomous Robots*, vol. 11, no. 3, pp. 207–213, 2001.

[3] U. Saranli, M. Buehler, and D. E. Koditschek, "Rhex: A simple and highly mobile hexapod robot," *The International Journal of Robotics Research*, vol. 20, no. 7, pp. 616–631, 2001.

[4] Y. Or and M. Moravia, "Analysis of foot slippage effects on an actuated spring-mass model of dynamic legged locomotion," *International Journal of Advanced Robotic Systems*, vol. 13, no. 2, p. 69, 2016. [Online]. Available: https://doi.org/10.5772/62687

[5] D. Zhao and S. Revzen, "Multi-legged steering and slipping with low dof hexapod robots," *Bioinspiration Biomimetics*, vol. 15, 2020.

[6] N. Neville, M. Buehler, and I. Sharf, "A bipedal running robot with one actuator per leg," in *Proceedings 2006 IEEE International Conference on Robotics and Automation, 2006. ICRA 2006.*, 2006, pp. 848–853.

[7] U. Saranli, M. Buehler, and D. E. Koditschek, "Rhex: A simple and highly mobile hexapod robot," *The International Journal of Robotics Research*, vol. 20, no. 7, pp. 616–631, 2001.

[8] F. Al-Bender, V. Lampaert, and J. Swevers, "The generalized maxwell-slip model: A novel model for friction simulation and compensation," *Automatic Control, IEEE Transactions on*, vol. 50, pp. 1883 – 1887, 12 2005.

[9] R. A. Romano and C. Garcia, "Karnopp friction model identification for a real control valve," *IFAC Proceedings Volumes*, vol. 41, no. 2, pp. 14 906–14 911, 2008, 17th IFAC World Congress. [Online]. Available: https://www.sciencedirect.com/science/article/pii/S1474667016413881

[10] J. Bastien, G. Michon, L. Manin, and R. Dufour, "An analysis of the modified dahl and masing models: Application to a belt tensioner," *Journal of Sound and Vibration*, vol. 302, no. 4, pp. 841–864, 2007. [Online]. Available: https://www.sciencedirect.com/science/article/pii/S0022460X06009126

[11] A. Saha, P. Wahi, M. Wiercigroch, and A. Stefanski, "A modified lugre friction model for an accurate prediction of friction force in the pure sliding regime," *International Journal of Non-Linear Mechanics*, vol. 80, 09 2015.

[12] T. Senoo and M. Ishikawa, "Analysis of sliding behavior of a biped robot in centroid acceleration space," *Robotica*, vol. -1, pp. 1–18, 09 2015.

[13] S. Andersson, "4 - friction and wear simulation of the wheel–rail interface," in *Wheel–Rail Interface Handbook*, R. Lewis and U. Olofsson, Eds. Woodhead Publishing, 2009, pp. 93–124. [Online]. Available: https://www.sciencedirect.com/science/article/pii/B9781845694128500045

[14] N. V. Rao, "Analysis of an actuated two segment leg model of locomotion," Master's thesis, Purdue University, 2013.

[15] E. Moore, D. Campbell, F. Grimminger, and M. Buehler, "Reliable stair climbing in the simple hexapod'rhex'," in *Proceedings 2002 IEEE International Conference on Robotics and Automation (Cat. No. 02CH37292)*, vol. 3. IEEE, 2002, pp. 2222–2227.

[16] R. Altendorfer, N. Moore, H. Komsuoglu, M. Buehler, H. Brown, D. McMordie, U. Saranli, R. Full, and D. E. Koditschek, "Rhex: A biologically inspired hexapod runner," *Autonomous Robots*, vol. 11, no. 3, pp. 207–213, 2001.

VI. APPENDIX

All the simulation code is uploaded on LCRS GitLab.